ELSEVIER

Chemical Geology 164 (2000) 1–20

CHEMICAL GEOLOGY
INCLUDING
ISOTOPE GEOSCIENCE

www.elsevier.com/locate/chemgeo

Salts of aliphatic carboxylic acids: Raman spectra and ion pairing in hydrothermal solutions containing sodium and calcium acetates

John D. Frantz *

Geophysical Laboratory, Carnegie Institution of Washington, Washington, DC 20015-1305, USA

Received 26 May 1998; accepted 28 May 1999

Abstract

A 2.0 molal solution of sodium acetate and 0.1, 0.5, and 1.0 molal solutions of calcium acetate were investigated by Raman spectroscopy from 22 to 400°C at 1000 and 2000 bar. Experiments were performed in a special hydrothermal pressure vessel fitted with conical diamond windows. In the case of the sodium acetate solution, perturbations of the internal vibrational modes of the acetate ligand resulting from the formation of sodium acetate ion pairs were undetectable. In the case of calcium acetate, however, the OCO bending mode, the C–C symmetric stretching mode, and the C–O symmetric stretching mode all showed evidence of ion pairing between calcium and acetate. The degree of formation of the ion pairs increased with increasing temperature, increasing concentration, and decreasing pressure. Mass action constants were calculated for the reaction involving Ca^{2+}, CH_3COO^-, and $CaCH_3COO^+$ which compare favorably with theoretically derived constants and with values derived from solubility experiments. The solutions existed metastably until temperatures approaching 480°C at which the acetate ligands underwent decarboxylation resulting in the formation of bicarbonate and methane. Combining mass action constants derived from this study with constants derived from the literature, distributions of the aqueous species were computed for the experimental conditions of the spectral measurements. © 2000 Elsevier Science B.V. All rights reserved.

Keywords: Raman spectroscopy; Acetate; Hydrothermal

1. Introduction

The presence of organic acids under subsurface conditions has been documented by its association with oil-field brines at temperatures approaching 200°C and the association of condensed organic material with sedimentary ore deposits which formed hydrothermally at temperatures up to 250°C (Giordano, 1993; Shock, 1993). Of the saturated acyclic aliphatic monocarboxylic acids and their associated salts, acetates, propanoates, and butanoates have been shown to be the most abundant in oil-field brines at temperatures above 100°C (Sverjensky, 1984). These acids are, however, metastable under subsurface conditions reacting with the breaking of the carbon–carbon bond (decarboxylation) to form carbon dioxide and methane (Kharaka et al., 1983). Palmer and Drummond (1986), in their study of thermal decarboxylation of acetate, studied the kinet-

* Fax: +1-202-686-2419; e-mail: frantz@gl.ciw.edu

0009-2541/00/$ - see front matter © 2000 Elsevier Science B.V. All rights reserved.
PII: S0009-2541(99)00137-0

ics of decarboxylation and the role of catalysis. Their results interpreted by Drummond and Palmer (1986) demonstrated that ''acetate can survive moderate hydrothermal temperatures (< 300°C) long enough to promote mobility of metals as acetate complexes.'' It is, therefore, important to consider the presence of aliphatic acids and their associated salts in modeling subsurface hydrothermal fluids associated with organic material.

Considerable attention has been given towards the experimental determination of the relative stabilities of acetate complexes under hydrothermal temperatures and pressures. Palmer and Drummond (1988) used potentiometric methods in their study of stability constants of ferrous acetate complexes at elevated temperatures and pressures. Ellis (1963) determined the ionization of acetic acid from conductance measurements to 225°C. Speciation in solutions containing acetic acid were studied to 275°C at 90 bar using Raman spectroscopy by Semmler and Irish (1988). Semmler et al. (1990) investigated complexing in magnesium acetate solutions to 250°C at 90 bar. Yang et al. (1989) spectroscopically identified lead and zinc acetate complexes in solutions at temperatures to 250°C and pressures to 110 bar. Giordano (1989) determined stability constants for lead acetate complexes to 85°C in his lead sulfate solubility studies. Seewald and Seyfried (1991) in their study of the solubility of portlandite in acetate solutions from 100 to 350°C at 500 bar retrieved stability constants for $CaCH_3COO^+$ from solubility data. Shock and Koretsky (1993) estimated the thermodynamic properties of acetate complexes and their relative stabilities based on existing experimental data and correlation algorithms.

The present study focuses on the determination of the behavior of sodium and calcium acetate solutions as a function of temperature and pressure. As in the case of Yang et al. (1989) and Semmler et al. (1990), Raman spectroscopy is used both to identify com-

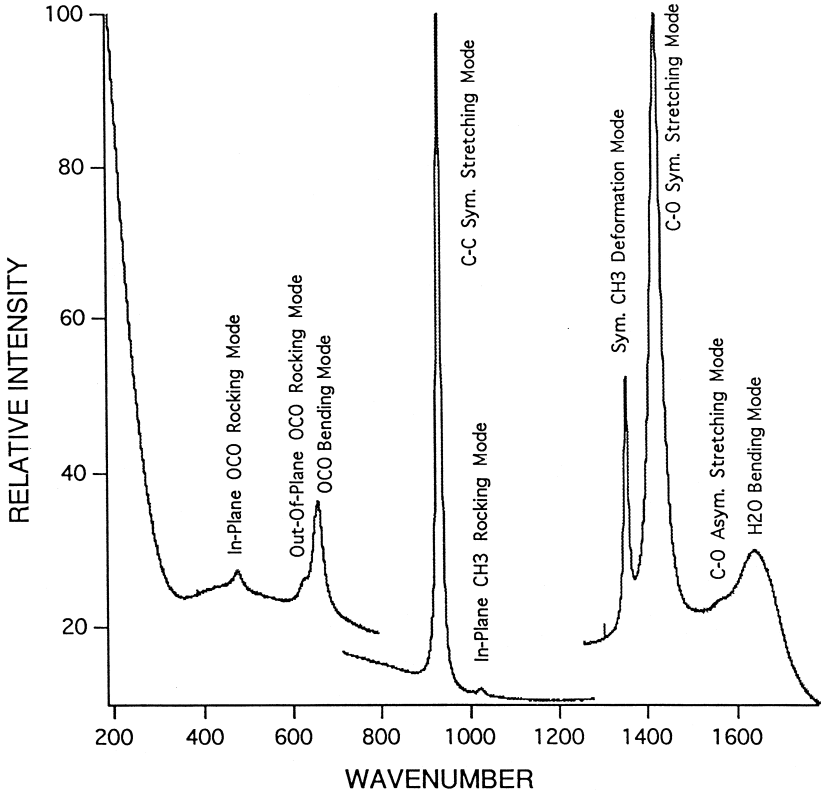

Fig. 1. Raman spectra of a 2 molal sodium acetate solution at 25°C and 1 atm. Not shown are the CH_3 symmetric and asymmetric stretching modes occurring at frequencies between 2900 and 3000 cm^{-1}.

plexes and determine mass action constants describing their relative concentrations. The behavior of calcium acetate solutions is of particular interest due to the influence that acetate potentially has on the chemistry of carbonate fluids determining the stability of carbonate cements (i.e., calcite) in sedimentary basins and on the chemistry of ore-forming hydrothermal fluids.

2. Experimental methods

The Raman spectra of sodium and calcium-bearing aqueous solutions were collected using a specially designed hydrothermal pressure vessel with diamond windows (Frantz, 1981; Frantz et al., 1993). The disk-shaped pressure vessel (diameter: 2 in.; height: 1 in.) contains two conical low-fluorescence diamond windows set at right angles to one another. The cell, containing a $Pt–Pt_{90}Rh_{10}$ thermocouple extending into the fluid cavity, is heated using two spirally wound platinum resistance furnace elements. The fluid is introduced and pressure is generated using a small stainless-steel intensifier. Pressure is measured using an Autoclave® 0–60,000 psi transducer. Pressure calibration of the transducer was accomplished using a recently calibrated Heise® bourdin-tube gauge. A melting point furnace was

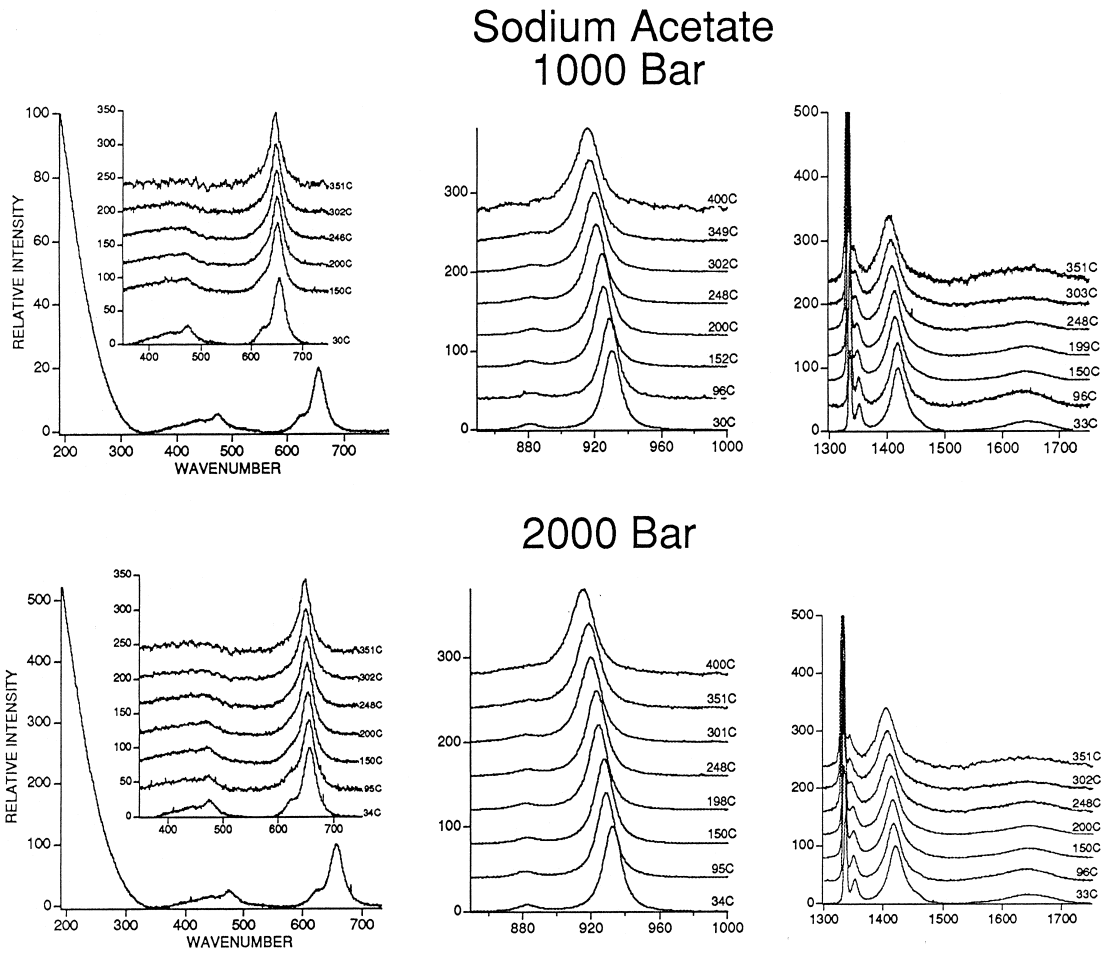

Fig. 2. Raman spectra of a 2 molal sodium acetate solution as a function of temperature (°C) at pressures of 1000 and 2000 bar. Three spectral ranges are shown.

Table 1
Results of deconvolutions

1.0 Molal Calcium Acetate Solution (1000 Bar)

192–792 range	Temp (°C)	Freq(1)	Area(1)	Width(1)	Freq(2)	Area(2)	Width(2)	Freq(3)	Area(3)	Width(3)
	22	621.1	122	21.4	655.8	576	28.1	675.6	91	18.0
	96	623.0	101	24.1	654.8	455	28.4	674.6	88	16.1
	145	623.4	94	27.9	653.5	359	28.0	673.4	120	20.2
	199	628.6	133	44.5	653.0	214	26.9	671.8	88	17.6
	249	631.0	140	63.1	650.7	96	24.4	670.0	77	20.0

710–1275 range	Temp (°C)	Freq(4)	Area(4)	Width(4)	Freq(5)	Area(5)	Width(5)	Freq(6)
	24	936.0	1263 (43)	12.5	942.8	524 (45)	11.7	na
	53	935.4	1252 (28)	13.0	942.9	647 (28)	11.6	na
	79	934.6	1158 (24)	13.2	942.4	707 (24)	11.8	na
	98	933.7	1177 (27)	13.6	941.8	857 (27)	12.4	na
	130	932.5	620	14.2	941.0	654	13.1	na
	163	931.2	576	14.7	940.1	580	14.2	na
	189	930.1	489	16.0	939.2	562	14.7	na
	248	922.5	217	18.1	932.3	321	14.1	942.9
	302	921.3	107	23.5	931.5	201	15.0	942.5
	352	917.7	63	33.5	929.4	96	15.6	940.2

1254–1783 range	Temp (°C)	Freq(7)	Freq(8)	Freq(9)	Area(9)	Width(9)	Freq(10)	Area(10)	Width(10)
	22	1335.5	1352.2	1419.9	3470	30.9	1442.5	827	33.2
	96	1335.8	1352.8	1419.4	1859	33.9	1442.5	637	38.6
	145	1333.9	1351.2	1416.6	1080	35.9	1439.4	490	40.4
	198	1333.8	1351.1	1415.2	490	37.5	1437.3	361	43.2
	248	1331.7	1349.9	1412.6	245	40.4	1434.7	291	49.2

1.0 Molal Calcium Acetate Solution (2000 Bar)

192–792 range	Temp (°C)	Freq(1)	Area(1)	Width(1)	Freq(2)	Area(2)	Width(2)	Freq(3)	Area(3)	Width(3)
	28	621.1	114	20.4	656.6	672	28.2	675.6	89	18.6
	96	622.1	102	24.6	655.3	554	28.7	675.0	89	16.9
	145	na	na	na	653.6	370	23.8	671.9	104	16.7
	200	na	na	na	653.1	285	26.6	672.3	92	18.1
	248	623.5	81	51.2	651.9	191	30.0	671.8	73	19.8
	303	622.1	38	51.6	649.0	97	28.7	670.2	66	24.0

710–1275 range	Temp (°C)	Freq(4)	Area(4)	Width(4)	Freq(5)	Area(5)	Width(5)	Freq(6)
	24	936.9	1370 (49)	13.0	943.4	436 (50)	11.8	na
	53	936.3	1358 (32)	13.4	943.4	591 (31)	11.6	na
	75	935.7	1331 (29)	13.4	943.1	664 (28)	11.7	na
	98	934.6	1331 (27)	13.6	942.4	753 (26)	11.9	na
	129	933.7	831 (20)	14.3	941.9	637 (21)	12.4	na
	163	932.3	721	14.8	940.9	742	13.4	na
	190	931.1	597	15.4	940.0	577	14.3	na
	248	924.2	263	17.3	933.8	423	15.6	na
	304	921.7	175	19.7	931.7	268	14.4	942.2
	350	920.3	103	25.8	931.0	157	15.0	942.0

Table 1 (continued)

1.0 Molal Calcium Acetate Solution (2000 Bar)

1254–1783 range	Temp (°C)	Freq(7)	Freq(8)	Freq(9)	Area(9)	Width(9)	Freq(10)	Area(10)	Width(10)
	28	1335.7	1352.7	1420.3	3448	30.2	1441.6	989	35.7
	98	1334.8	1351.9	1418.8	2207	33.0	1441.6	661	36.4
	144	1335.0	1352.3	1418.1	1321	35.0	1440.5	533	39.2
	199	1333.0	1350.5	1415.0	712	38.0	1437.1	418	43.0

0.1 Molal Calcium Acetate Solution (1000 Bar)

710–1275 range	Temp (°C)	Freq(4)	Area(4)	Width(4)	Freq(5)	Area(5)	Width(5)	Freq(6)
	28	936.8	1087	13.4	na	na	na	na
	52	936.1	1058	13.7	na	na	na	na
	74	935.2	1000	13.8	944.3	27	6.9	na
	99	934.2	744	13.6	943.5	40	7.5	na
	121	932.5	515 (15)	13.9	942.1	54 (9)	8.8	na
	151	931.3	333 (11)	14.2	941.4	85 (10)	9.6	na
	179	930.1	265 (12)	14.8	940.4	78 (9)	10.6	na
	199	929.3	242 (12)	16.8	940.0	64 (6)	9.5	na
	230	927.2	118 (16)	19.1	938.3	106 (28)	12.6	na
	253	926.0	115	20.4	937.2	135	13.1	na

0.1 Molal Calcium Acetate Solution (2000 Bar)

710–1275 range	Temp (°C)	Freq(4)	Area(4)	Width(4)	Freq(5)	Area(5)	Width(5)	Freq(6)
	28	937.7	971	13.6	na	na	na	na
	50	937.1	957	14.0	na	na	na	na
	72	936.2	888	14.2	na	na	na	na
	94	935.5	674	14.6	na	na	na	na
	121	933.8	480 (15)	15.2	943.7	30 (9)	8.2	na
	152	932.5	363 (9)	14.8	943.1	35 (4)	7.0	na
	179	931.2	260 (15)	15.2	941.6	88 (16)	9.5	na
	200	930.3	205 (10)	16.6	941.0	62 (9)	9.7	na
	231	928.7	159 (21)	18.6	939.7	87 (31)	9.5	na
	253	927.4	87 (14)	20.7	938.1	62 (11)	11.2	na

0.5 Molal Calcium Acetate Solution (1000 Bar)

710–1275 range	Temp (°C)	Freq(4)	Area(4)	Width(4)	Freq(5)	Area(5)	Width(5)	Freq(6)
	24	936.5	1891	14.5	na	na	na	na
	50	934.5	1397 (30)	12.7	941.8	449 (30)	10.7	na
	73	933.8	1470 (21)	12.9	941.6	406 (19)	10.5	na
	104	932.9	1120 (15)	13.3	941.2	415 (14)	10.7	na
	128	931.8	996 (14)	13.8	940.6	446 (12)	11.3	na
	152	930.7	761 (13)	13.8	939.7	523 (13)	11.8	na
	175	929.7	625 (12)	14.5	939.0	529 (12)	12.4	na
	200	928.7	448	15.1	938.4	482	12.9	na
	226	927.6	384	15.8	937.6	383	13.8	na
	250	926.2	247	16.6	936.7	328	14.8	na

0.5 Molal Calcium Acetate Solution (2000 Bar)

710–1275 range	Temp (°C)	Freq(4)	Area(4)	Width(4)	Freq(5)	Area(5)	Width(5)	Freq(6)
	25	937.2	1914	14.4	na	na	na	na
	49	936.5	1502 (31)	15.0	942.0	409 (31)	12.6	na

Table 1(continued)

1.0 Molal Calcium Acetate Solution (2000 Bar)

710–1275 range	Temp (°C)	Freq(4)	Area(4)	Width(4)	Freq(5)	Area(5)	Width(5)	Freq(6)
	72	934.8	1468 (22)	13.1	942.1	399 (21)	10.4	na
	104	933.8	1256 (16)	13.4	941.7	368 (14)	10.6	na
	127	932.9	1098 (16)	13.7	941.2	410 (14)	10.9	na
	152	931.9	937 (14)	14.1	940.6	443 (13)	11.4	na
	175	931.0	808 (12)	14.7	939.9	445 (11)	11.7	na
	201	929.8	640 (14)	15.1	939.1	492 (13)	12.5	na
	224	928.7	439	15.6	938.4	473	12.9	na
	250	927.6	398	16.4	937.6	357	13.7	na

2.0 Molal Sodium Acetate Solution (1000 Bar)

192–792 range	Temp (°C)	Freq(1)	Area(1)	Width(1)	Freq(2)	Area(2)	Width(2)
	30	620.9	71	21.9	655.1	533	26.4
	97	na	na	na	653.5	409	28.1
	150	621.2	65	27.9	651.4	503	25.9
	200	623.6	65	32.1	651.2	453	25.5
	246	623.9	73	41.5	650.0	403	25.0
	302	624.0	86	57.1	648.6	300	23.4
	351	na	na	na	646.8	158	22.5

710–1275 range	Temp (°C)	Freq(4)	Width(4)
	30	930.2	12.3
	96	928.7	12.0
	152	925.0	12.4
	200	924.2	13.0
	248	920.5	13.8
	302	919.3	15.1
	349	916.3	15.6
	400	915.2	16.9

1254–1783 range	Temp (°C)	Freq(7)	Freq(8)	Area(8)	Width(8)	Freq(9)	Area(9)	Width(9)
	33	1335.4	1351.4	444	10.5	1418.4	2926.4	29.0
	96	1335.6	1351.7	192	9.6	1417.0	1349.0	29.1
	150	1333.3	1349.6	155	10.3	1412.8	1264.8	32.7
	199	1333.8	1349.9	99	9.2	1412.1	1090.3	36.5
	248	1331.6	1347.7	76	9.6	1408.1	891.6	39.0
	303	1331.8	1346.1	82	11.7	1406.2	755.8	38.6
	351	1329.3	1343.4	34	10.0	1402.9	398.1	40.7
	400	1329.4	1343.9	3	4.1	1406.5	123.1	53.9

2.0 Molal Sodium Acetate Solution (2000 Bar)

192–792 range	Temp (°C)	Freq(1)	Area(1)	Width(1)	Freq(2)	Area(2)	Width(2)
	34	620.7	73	22.4	656.2	563	27.3
	95	622.2	115	38.1	654.7	505	26.5
	150	622.7	74	30.4	653.1	490	26.3
	200	623.2	78	36.9	651.9	444	25.9
	248	623.3	57	36.5	651.1	416	25.4
	302	624.3	64	49.9	649.9	326	24.9
	351	na	na	na	648.1	219	24.5
	400	na	na	na	645.8	100	23.2

Table 1(continued)

1.0 Molal Calcium Acetate Solution (1000 Bar)

710–1275 range	Temp (°C)	Freq(4)	Width(4)
	34	932.2	12.4
	95	928.5	12.2
	150	927.3	12.5
	198	924.0	13.1
	248	922.8	13.9
	301	919.4	14.8
	351	918.2	15.5
	400	914.7	16.7

1254–1783 range	Temp (°C)	Freq(7)	Freq(8)	Area(8)	Width(8)	Freq(9)	Area(9)	Width(9)
	33	1336.5	1352.9	332	9.7	1419.9	2375	28.5
	96	1334.5	1350.9	238	9.6	1416.7	1888	30.2
	150	1334.7	1351.4	155	10.2	1415.1	1319	32.8
	200	1334.1	1350.9	146	11.8	1412.5	1017	33.5
	248	1332.6	1349.5	72	10.6	1410.1	829	41.1
	302	1330.7	1345.6	95	11.9	1406.0	841	38.9
	351	1330.5	1345.0	52	11.4	1404.6	511	40.3
	400	1328.4	1343.8	13	8.0	1401.8	197	42.2

Where: Peak(1): Out-of-Plane OCO rocking mode, Peak(2): OCO bending mode (unbound acetate), Peak(3): OCO bending mode (bound acetate), Peak(4): C–C symmetric stretching mode (unbound acetate), Peak(5): C–C symmetric stretching mode (bound acetate), Peak(6): C–C symmetric stretching mode (bound acetate), Peak(7): C–C symmetric stretching mode (diamond), Peak(8): symmetric CH_3 deformation mode, Peak(9): symmetric C–O stretching mode (unbound acetate), Peak(10): symmetric C–O stretching mode (bound acetate).

used in the temperature calibration of the thermocouples. Temperature errors are thought to be ± 5°C; pressure errors, ± 10 bar. The pressure vessel and much of the pressure-generating apparatus are gold plated to reduce the effects of corrosion and therefore inhibit fluorescence. Prior to use, the cell and associated pressure-generating apparatus were repeatedly cleaned with ultra-pure hexane, methanol, and triple-distilled water. Great care was taken in filling the system with the sample fluid in order to prevent the introduction of dust and bubbles.

The optical cell was used in conjunction with a Dilor® XY confocal Raman spectrometer equipped with CCD detector. Gratings with 1800 lines/mm yield a spectral resolution of approximately 1 cm^{-1}. The 514.5 nm line of a SpectroPhysics® model 2025 Ar^+ laser operating at 1.8 W was used for sample excitation. The spectrometer was calibrated with respect to wavenumber using both the frequency of the laser line and a mercury lamp. Collection of the scattered light was at 90° to the incident radiation. Experiments were performed by first incrementing temperature and measuring spectra at varying pressures. Signal collection times averaged 300 s. Analyses of the resulting Raman spectra were accomplished using computer algorithms contained in the software package *Igor Pro* (WaveMetrics®).

The 2.0 molal sodium acetate aqueous solution was prepared from crystalline anhydrous sodium acetate reagent (Alfa®, Stock #11554, Lot #F13G02) and doubly distilled water; the 0.1, 0.5, and 1.0 molal calcium acetate solutions, from hydrous calcium acetate powder (Alfa®, Stock #13446, Lot #082180). The solutions used in the experiments were prepared by mixing solutions with concentrations higher than those desired, performing sodium or calcium analyses of these using atomic absorption spectrometry, and diluting these to the desired molality.

3. Spectral assignments

Acetate, an acyclic aliphatic framework molecule, is composed of a carboxyl group and a single methyl

group. As an unbound aqueous ligand, the acetate ion exhibits C_{2v} symmetry with 15 vibrational modes (Kaklhana et al., 1983). The primary modes of the carboxyl group are the OCO in-plane rocking mode ($\gamma_{in(OCO)}$), the OCO out-of-plane rocking mode ($\pi_{(OCO)}$), the OCO in-plane bending mode ($\delta_{(OCO)}$), and the symmetric ($\nu_{s(CO)}$) and antisymmetric ($\nu_{as(CO)}$) C–O symmetric stretching modes. The methyl group exhibits a symmetric ($\nu_{s(CH_3)}$) and asymmetric ($\nu_{as(CH_3)}$) CH_3 stretching mode, a CH_3 stretching mode ($\nu_{(CH_3)}$), in- ($\gamma_{in(CH_3)}$) and out-of-plane ($\pi_{(CH_3)}$) CH_3 rocking modes, symmetric ($\delta_{s(CH_3)}$) and asymmetric ($\delta_{as(CH_3)}$) deformation modes, an additional deformation mode ($\delta_{(CH_3)}$) and a torsion mode ($\tau_{(CH_3)}$). The C–C symmetric stretching mode ($\nu_{(C-C)}$) represents a fundamental vibrational mode resulting from the interaction of the carboxyl and methyl groups. Of these modes, only eight are discernible in our Raman spectra of a 2 molal solution of sodium acetate collected between 192 and 1783 cm^{-1} at 25°C, 1 atm (Fig. 1). The in-plane OCO rocking mode occurs at 476 cm^{-1}; the out-of-plane OCO rocking mode, at 628 cm^{-1}; the OCO in-plane bending mode, at 657 cm^{-1}; the C–C symmetric stretching mode, at 931 cm^{-1}; the CH_3 in-plane rocking mode, at 1023 cm^{-1}; the CH_3 symmetric deformation mode, at 1352 cm^{-1}; the C–O symmetric stretching mode, at 1419 cm^{-1}; and the C–O asymmetric stretching mode at 1561 cm^{-1}. The out-of-plane CH_3 rocking mode is indiscernible. The asymmetric CH_3 deformation mode is obscured by the C–O symmetric stretching mode.

The association of cations with complex ligands can occur as solvent-separated ion pairs (outer-sphere complexes) or direct cation–anion contact pairs (inner sphere complexes). Solvent-separated ion pairs, due to the separation of the cations and anions by waters of solvation, have little effect on the Raman spectra of the complex ligand. Contact-pairs, however, do affect the internal modes of the ligand. The coordination of the association of cations with the acetate ligand as contact ion pairs (inner-sphere complexes) is difficult to assess based on the results of Raman studies without complementary X-ray and NMR studies. Possibilities include monodentate association of the cation with one oxygen, bidentate association of the cation with two oxygens, and a bridged association of two cations with the two oxygens of the carboxyl group (Yang et al., 1989). Such relatively weak associations serve to perturb the existing symmetry of the complex ligand causing existing bands to split. Due to the direct association of the cation with the carboxyl group of the acetate complex, the carboxyl vibrational modes and the mode associated with the carbon–carbon bond can be expected to most affected.

4. Experimental results

4.1. Spectroscopy

Previous studies involving ion pairing of alkalis with complex ligands in relatively dilute solutions (Spohn and Brill, 1989; Frantz, 1998) have shown that association has undramatic, if noticeable, effects on the frequencies or half-widths of the internal modes of the ligands. This is probably due to alkalis cations primarily forming solvent-separated ion pairs. Association of alkaline earths with complex ligands (which probably form contact ion pairs due to their larger charge density), have been demonstrated to affect the internal modes of the ligands (Semmler et al., 1990; Frantz et al., 1994). In order to identify and analyze spectral perturbations due to ion-pairing, experiments were done for both sodium acetate and calcium acetate solutions.

Experiments were performed on a 2.0 molal sodium acetate solution as a function of temperature at both 1000 and 2000 bar pressure (Fig. 2). Spectra were collected in three frequency ranges: 192–792, 710–1275, and 1254–1783 cm^{-1}. The spectra were corrected for the Bose–Einstein effect (Long, 1977) and for background using fourth- or fifth-order polynomials. The frequencies and half-widths of the major bands are presented in Table 1 and in Fig. 3. The frequencies systematically decrease; the half-widths of the C–C symmetric stretch and the C–O symmetric stretch systematically increase with increasing temperature for both 1000 and 2000 bar. The half-widths of the OCO bending mode decrease with increasing temperature. The peak at 1330 cm^{-1} (as seen in Fig. 2, corresponds to the C–C symmetric stretch of the diamond window of the optical cell. Solutions remained stable for 24-h periods with no sign of decarboxylation. Decarboxylation did occur

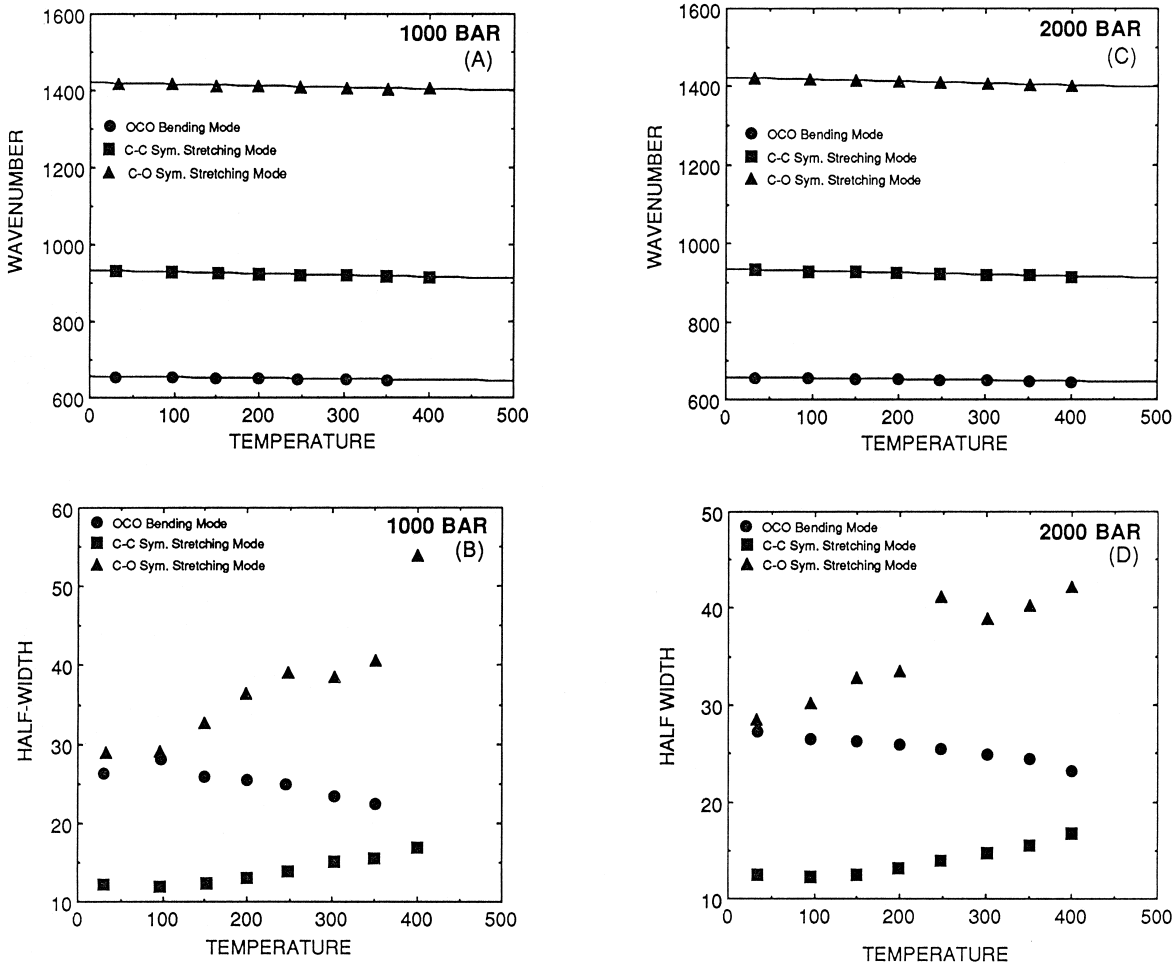

Fig. 3. Frequencies and half-widths of sodium acetate bands.

(within seconds) at approximately 480°C resulting in the appearance peaks indicating the presence of both bicarbonate and methane (Fig. 4). The spectra in Fig. 4 were taken after lowering the temperature to approximately 250°C to improve the signal to noise ratio and separate the bicarbonate peak from the acetate peak.

Experiments were carried out on 0.1, 0.5, and 1.0 molal calcium acetate solutions. The results of measurements on the 1.0 molal solution (after performing the corrections listed above) are shown in Fig. 5. Significant differences exist between the spectra of the 1.0 molal calcium acetate and the 2.0 molal sodium acetate solutions (Fig. 2). The OCO bending mode seen as a single peak in the case of sodium acetate (Fig. 2) has split into two peaks for calcium acetate with the peak at higher frequency increasing in intensity with respect to the lower frequency with increasing temperature. The C–C symmetric stretching mode identified as a single peak in the sodium acetate can be seen to have also split into two peaks again with the higher frequency peak increasing in relative intensity with respect to the lower frequency peak with increasing temperature. Similarly, the single C–O symmetric stretch shown in Fig. 2, for sodium acetate, follows the same trend. These trends were not discernible for the in- and out-of-plane rocking modes or the C–O asymmetric stretching

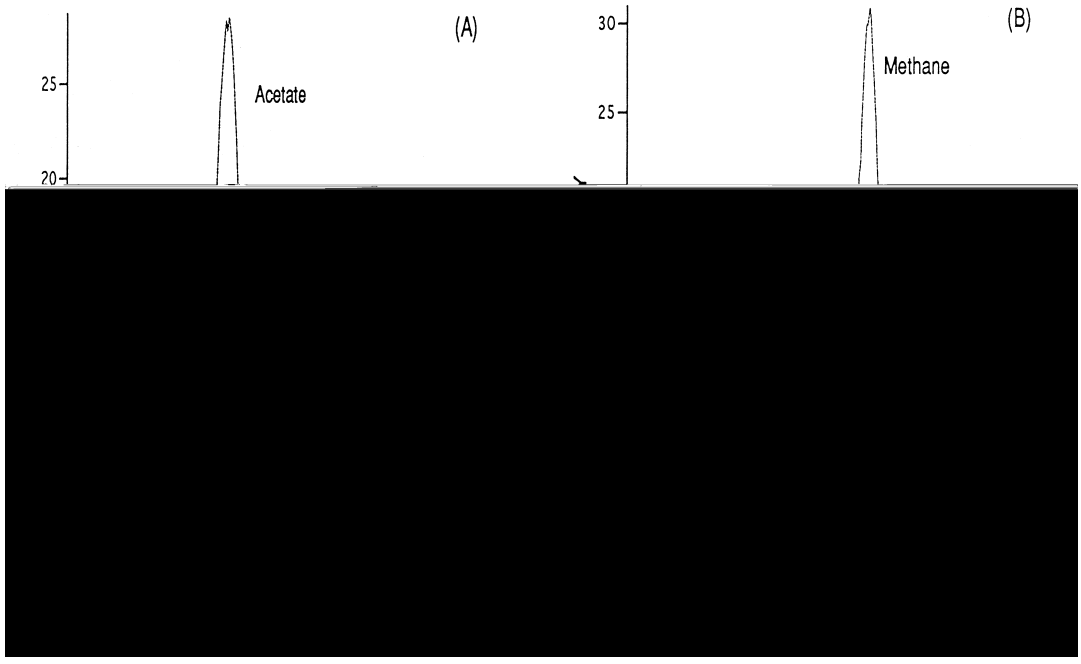

Fig. 4. Raman spectra of a 2-molal sodium acetate after decomposition at 480°C with subsequent cooling to 250°C.

mode due to their low intensities. The frequency and half-width of the symmetric CH_3 deformation mode is reasonably similar for both solutions and does not appear to split in the case of calcium acetate. The differences between the spectra of the 2 molal sodium acetate and the 1 molal calcium acetate solutions (both having a 2 molal concentration of the acetate ligand) are shown with the frequency ranges reduced in Fig. 6.

The spectral envelopes containing the OCO bending mode (594–712 cm^{-1}), the C–C symmetric stretch mode (880–988 cm^{-1}), and the C–O symmetric stretch mode (1310–1510 cm^{-1}) were deconvoluted using the software package *Igor Pro* (WaveMetrics®). In all cases, the spectral envelopes were fit using Lorenzian peak shapes with the number of bands being dictated by the inflections in the spectral envelopes. Results of the deconvolutions are presented in Table 1 and examples of these fits for calcium acetate are given in Fig. 7. Frequencies, areas and half-widths are given. In the case of the envelope containing the out-of-plane OCO rocking mode and the OCO bending mode, only three bands could be justifiably resolved. At low temperatures, the frequency of the lowest-frequency peak of the deconvolution corresponds to the out-of-plane OCO rocking mode for of the unbound acetate ligand as seen in the sodium acetate spectra. As temperature increases, however, its frequency increases rather than decreases probably indicating the presence of an unresolvable second out-of-plane OCO rocking mode band. The remaining two peaks are assigned to the OCO bending mode. Justification is based on comparison of the frequencies of the deconvoluted curves with those of sodium acetate bands (Fig. 8A,D). The frequency of the mid-frequency peak of the deconvolution for the 1 molal calcium acetate solution very closely matches that of the sodium acetate solution. The relatively high intensity of the third peak dictates that it also represents the bending mode rather than the out-of-plane rocking mode of the acetate ligand. Frequencies of the two bands representing the OCO bend systematically decrease with increasing temperature (Fig. 8A,D). Similar results can be seen from the deconvolution of the envelope containing the C–C stretch mode. The frequency of the lower

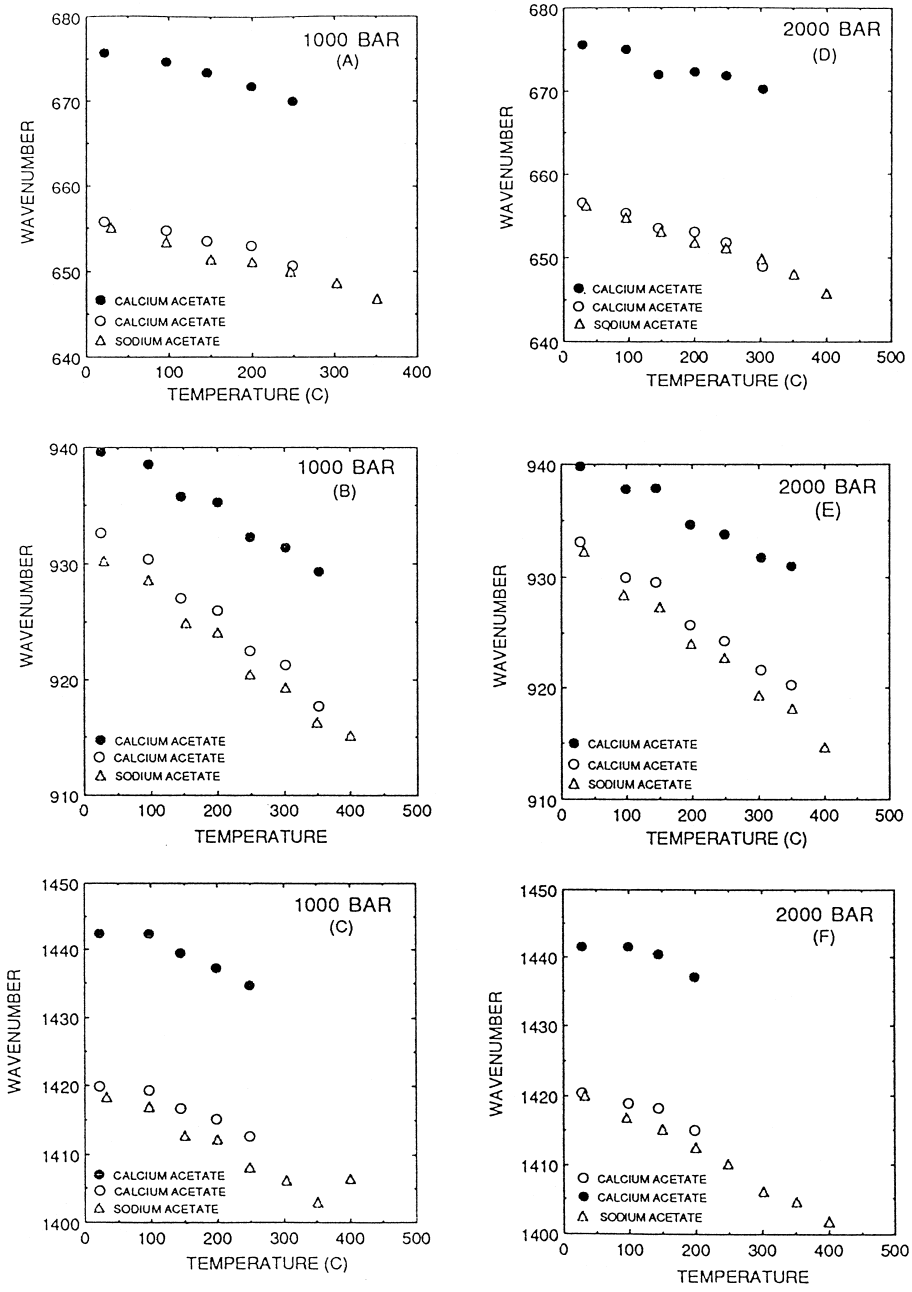

Fig. 8. Frequencies of deconvoluted spectral envelopes at 1000 and 2000 bar pressure. (A) and (D) refer to the OCO bending mode; (B) and (E), to the C–C symmetric stretch mode; (C) and (F), to the O–C symmetric stretch mode.

acetate solutions. As the internal modes of the acetate ligand are not measurably affected by the presence of sodium ions, the band positions for the acetate ions in sodium acetate solutions can represent both unbound acetate ions and sodium acetate ion-pairs. The lower-frequency components of the calcium acetate doublets, in each case, match the frequency of the corresponding single sodium acetate

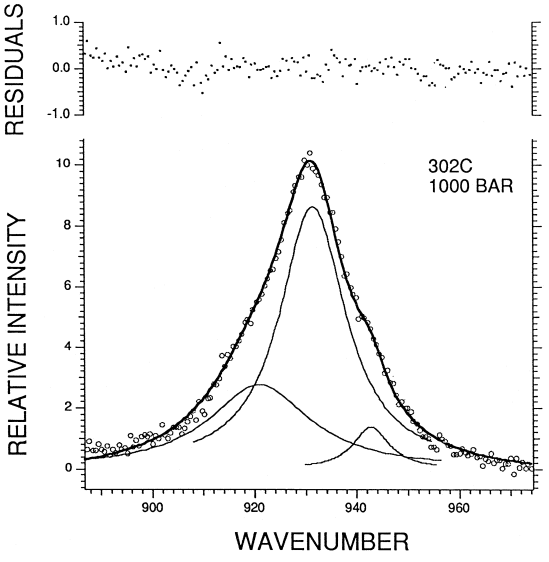

Fig. 9. Raman spectra of a 1 molal calcium acetate solution indicating the appearance of the neutral calcium acetate complex ($CaCH_3COO^{\cdot}$) at 302°C, 1000 bar.

bands (Fig. 8) and are therefore assumed to represent unbound acetate ions. The higher-frequency components would thus represent bound acetate. Assuming *stepwise* association constants for the species Ca^{2+}, $CaCH_3COO^+$, and $Ca(CH_3COO)_2^{\cdot}$:

$$Ca^{2+} + CH_3COO^- = CaCH_3COO^+ \quad (1)$$

$$CaCH_3COO^+ + CH_3COO^- = Ca(CH_3COO)_2^{\cdot} \quad (2)$$

the lower and higher frequency peaks in the doublets must represent CH_3COO^- and $CaCH_3COO^+$ ions, respectively.

The concentration of an aqueous species can be related to the integrated area of a Raman band according to the following expression:

$$m_i = f_i A_i \quad (3)$$

where m_i represents the molal concentration of the ith species; A_i, the area of the Raman peak representing the ith species; and f_i, the Raman scattering cross-section for the ith species. Dividing the concentration of bound acetate (representing $CaCH_3COO^+$) by that of unbound acetate (CH_3COO^-):

$$m_{CaCH_3COO^+}/m_{CH_3COO^-} = R\left(A_{CaCH_3COO^+}/A_{CH_3COO^-}\right) \quad (4)$$

where R is the ratio of the Raman scattering cross of $f_{CaCH_3COO^+}$ over $f_{CH_3COO^-}$ respectively and A_i represents the area of the ith species. Considering the mass balance expression for total acetate:

$$m_{CH_3COO(T)} = m_{CH_3COO^-} + m_{CaCH_3COO^+} + 2m_{Ca(CH_3COO)_2} \quad (5)$$

and assuming only minor concentrations of $Ca(CH_3COO)_2$, substitution of Eq. (4) into Eq. (5) yields an expression for the calculation of the molal concentration of CH_3COO^-:

$$m_{CH_3COO^-} = m_{CH_3COO(T)} / \left(1 + R\left(A_{CaCH_3COO^+}/A_{CH_3COO^-}\right)\right) \quad (6)$$

The molal concentration of $CaCH_3COO^+$ and Ca^{2+} are calculated from:

$$m_{CaCH_3COO^+} = m_{CH_3COO(T)} - m_{CH_3COO^-} \quad (7)$$

and

$$m_{Ca^{2+}} = m_{Ca(T)} - m_{CaCH_3COO^+} \quad (8)$$

where $m_{Ca(T)}$ is the total concentration of calcium in the solution.

The relative areas of the Raman in the doublets corresponding to CH_3COO^- and $CaCH_3COO^+$ are given in Table 1 for 0.1, 0.5, and 1.0 molal calcium acetate solutions. Errors corresponding to ± 1 standard deviation of the deconvoluted areas are in parentheses after the corresponding values in Table 1. Assuming that the scattering cross-sections for the peaks in the doublets to be equal, the calculated concentrations of the species are presented in Table 2. In the case of the 1.0 molal calcium acetate solution, the relative areas are given for the OCO bending mode, the C–C symmetric stretch mode, and the C–O symmetric stretch mode. For the 0.1 and 0.5 molal solutions, only data for the C–C symmetric stretch mode were measured. Only the area ratios for the C–C symmetric stretch mode were used as deconvolutions of both the OCO bending mode and the C–O symmetric stretching mode involved peaks from overlapping modes. In the case of the OCO bending mode, the observation made earlier that the frequency of the out-of-plane rocking mode increased with increasing temperature may indicate

Table 2
Association constant calculations $Ca^{2+} + CH_3COO^- = CaCH_3COO^+$

1000 Bar $Ca(CH_3COO)_2$ total molality	Temp (°C)	Ratio $CaAc^+/Ac^-$	CH_3COO^- (molal)	$CaCH_3COO^+$ (molal)	Ca^{2+} (molal)	Ionic strength	Log $\gamma_{Ca^{2+}}$	Log K
1.0	53	0.52	1.32	0.68	0.32	1.64	−0.66	0.87 (.07)
1.0	79	0.61	1.24	0.76	0.24	1.48	−0.69	1.09 (.07)
1.0	98	0.73	1.16	0.84	0.16	1.31	−0.73	1.40 (.09)
0.5	50	0.32	0.76	0.24	0.26	1.01	−0.64	0.74 (.06)
0.5	73	0.28	0.78	0.22	0.28	1.07	−0.68	0.67 (.04)
0.5	104	0.37	0.73	0.27	0.23	0.96	−0.69	0.90 (.04)
0.5	128	0.45	0.69	0.31	0.19	0.88	−0.72	1.09 (.04)
0.5	152	0.69	0.59	0.41	0.09	0.69	−0.74	1.61 (.06)
0.5	175	0.85	0.54	0.46	0.04	0.58	−0.77	2.07 (.11)
0.1	121	0.11	0.18	0.02	0.08	0.26	−0.59	0.70 (.10)
0.1	151	0.26	0.16	0.04	0.06	0.22	−0.59	1.22 (.10)
0.1	179	0.29	0.15	0.05	0.05	0.21	−0.61	1.35 (.11)
0.1	199	0.26	0.16	0.04	0.06	0.22	−0.67	1.32 (.09)
0.1	230	0.90	0.11	0.09	0.01	0.11	−0.58	2.81 (.69)
2000 Bar $Ca(CH_3COO)_2$ total molality	Temp (°C)	Ratio $CaAc^+/Ac^-$	CH_3COO^- (molal)	$CaCH_3COO^+$ (molal)	Ca^{2+} (molal)	Ionic strength	Log $\gamma_{Ca^{2+}}$	Log K
1.0	53	0.44	1.39	0.61	0.39	1.79	−0.71	0.76 (.07)
1.0	75	0.50	1.33	0.67	0.33	1.67	−0.76	0.93 (.06)
1.0	98	0.57	1.28	0.72	0.28	1.55	−0.79	1.09 (.06)
1.0	129	0.77	1.13	0.87	0.13	1.26	−0.83	1.59 (.10)
0.5	49	0.27	0.79	0.21	0.29	1.07	−0.62	0.60 (.06)
0.5	72	0.27	0.79	0.21	0.29	1.07	−0.66	0.63 (.05)
0.5	104	0.29	0.77	0.23	0.27	1.05	−0.67	0.70 (.03)
0.5	127	0.37	0.73	0.27	0.23	0.96	−0.70	0.91 (.04)
0.5	152	0.47	0.68	0.32	0.18	0.86	−0.72	1.14 (.04)
0.5	175	0.55	0.64	0.36	0.14	0.79	−0.76	1.34 (.04)
0.5	201	0.77	0.57	0.43	0.07	0.63	−0.77	1.84 (.09)
0.1	121	0.06	0.19	0.01	0.09	0.28	−0.65	0.50 (.17)
0.1	152	0.10	0.18	0.02	0.08	0.26	−0.58	0.66 (.08)
0.1	179	0.39	0.15	0.05	0.05	0.20	−0.57	1.41 (.18)
0.1	200	0.30	0.15	0.05	0.05	0.21	−0.61	1.36 (.13)
0.1	231	0.55	0.13	0.07	0.03	0.16	−0.59	1.49 (.08)
0.1	253	0.72	0.12	0.08	0.02	0.13	−0.60	2.60 (.37)

that additional peak(s) may contribute to the spectral envelope but not be resolvable. With respect to the envelope containing the symmetric C–O stretch, the presence of the antisymmetric CH_3 deformation complicates deconvolution. In addition, since the oxygens in the OCO bend and C–O stretching modes are intimately involved with the association of the acetate ligand with calcium, the assumption that the ratio of the scattering coefficients being unity is much less robust. Mass action constants were calculated for Eq. (1):

$$\text{Log } K = a_{CaCH_3COO^+}/a_{Ca^{2+}}a_{CH_3COO^-} \quad (9)$$

Assuming the activity coefficients of $CaCH_3COO^+$ ($\gamma_{CaCH_3COO^+}$) and CH_3COO^- ($\gamma_{CH_3COO^-}$) are equal (assuming the ion size parameters for the acetate ion and the calcium acetate ion-pair in the extended Debye–Huckel expression are approximately equal):

$$\text{Log } K = \left[m_{CaCH_3COO^+}/m_{Ca^{2+}}m_{CH_3COO^-}\right]\left[1/\gamma_{Ca^{2+}}\right] \quad (10)$$

where $\gamma_{Ca^{2+}}$ is the activity coefficient of calcium ion. The molal activity coefficient of calcium ion was computed using the ''B-dot'' equation as described in the work of Helgeson (1969). Debye–Huckel parameters were obtained from Helgeson and Kirkham (1974); the ion size parameter, from Klotz (1964). The computed ionic strengths, activity coefficients of calcium ion, and mass action constants for the three concentrations at 1000 and 2000 bar are given in Table 2. The numbers in parentheses listed after the values of Log K in Table 2 represent the errors in the calculated equilibrium constants due to the errors in the measurement of peak area (listed in Table 1). The calculated values for the logarithm (base 10) of the association constant (along with the associated errors) are shown as a function of inverse temperature (K) in Fig. 10 for 1000 and 2000 bar. The dashed lines represent an uncertainty of ± 1 standard deviation in the fitted line. While agreement is quite good, there is a reasonably small but systematic variation of the values of Log K with concentration. The origin of this trend is unknown. Values of activity coefficients, the Raman scattering coefficient ratio, line shapes used in spectral deconvolutions, etc. are all possibilities but, without further information, the cause of this uncertainty remains uncertain.

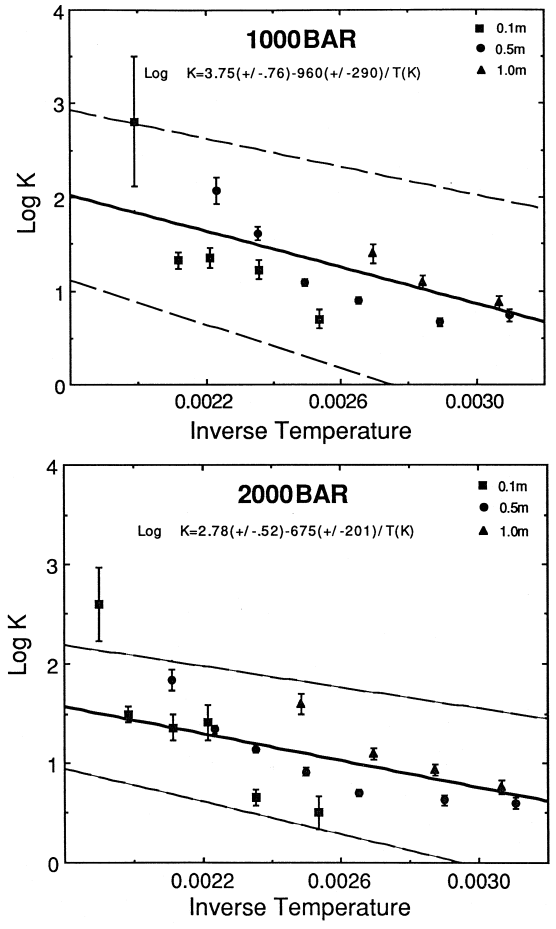

Fig. 10. Computed association constants at both 1000 and 2000 bar pressure for the equilibrium: $Ca^{2+} + CH_3COO^- = CaCH_3COO^+$. Error bars are plotted for individual data points. The solid lines represent weighted regressions of the data. The dashed lines represent an error of ± 1 standard deviation for these fitted lines.

In Fig. 11, the values of the logarithm of the association constant at 1000 and 2000 bar (this work) and the experimentally determined value at 500 bar (Seewald and Seyfried, 1991) at 200°C are plotted as a function of the logarithm of the density of water. Plots such as these have been demonstrated to be linear for association constants (Quist and Marshall, 1968). The data appear to be reasonably consistent. The errors for the 1000 bar and 2000 bar data represent the errors for the fitted line of the association constant shown in Fig. 10. No errors are available for the data of Seewald and Seyfried (1991) but

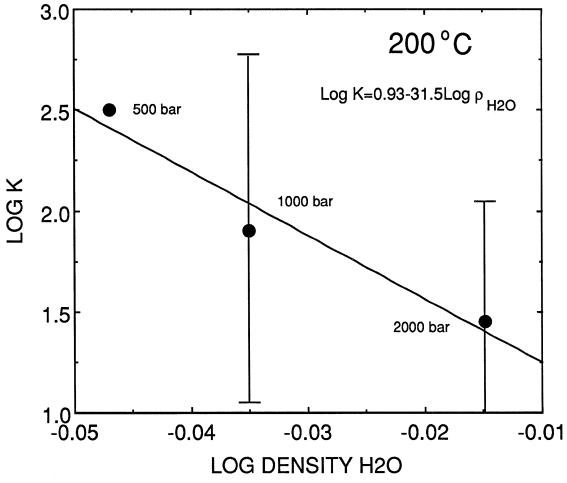

Fig. 11. Comparison of the results of these experiments at 1000 and 2000 bar with the result of Seewald and Seyfried (1991) at 500 bar. Error bars representing ± 1 standard deviation of the fitted line shown in Fig. 10 are plotted for these experiments. No errors were provided by Seewald and Seyfried (1991). The line is fitted through the experimental data both of this work and that of Seewald and Seyfried (1991).

are probably large due to the fact that retrieval of their data involved the simultaneous solution of a number of mass action expressions. Significant uncertainty exists for each of the mass action constants associated with these expressions. Shock and Koretsky (1993) theoretically estimated values of the logarithm of the mass action constant. Their values at 200°C are 2.27, 2.16, and 2.02 at 500, 1000, and 2000 bar, respectively. Their estimates appear to show a reduced effect of pressure on the values of the association constants. Calculation of species distributions and mass action constants were restricted to temperature–pressure conditions at which the relative area of the peak representing $CaCH_3COO^+$ was less than that of the peak representing CH_3COO^-. At higher temperature conditions at which the area of calcium acetate exceeds that of acetate, it is assumed that the concentration of the neutral species $Ca(CH_3COO)_2^{\circ}$ is becoming important. This assump-

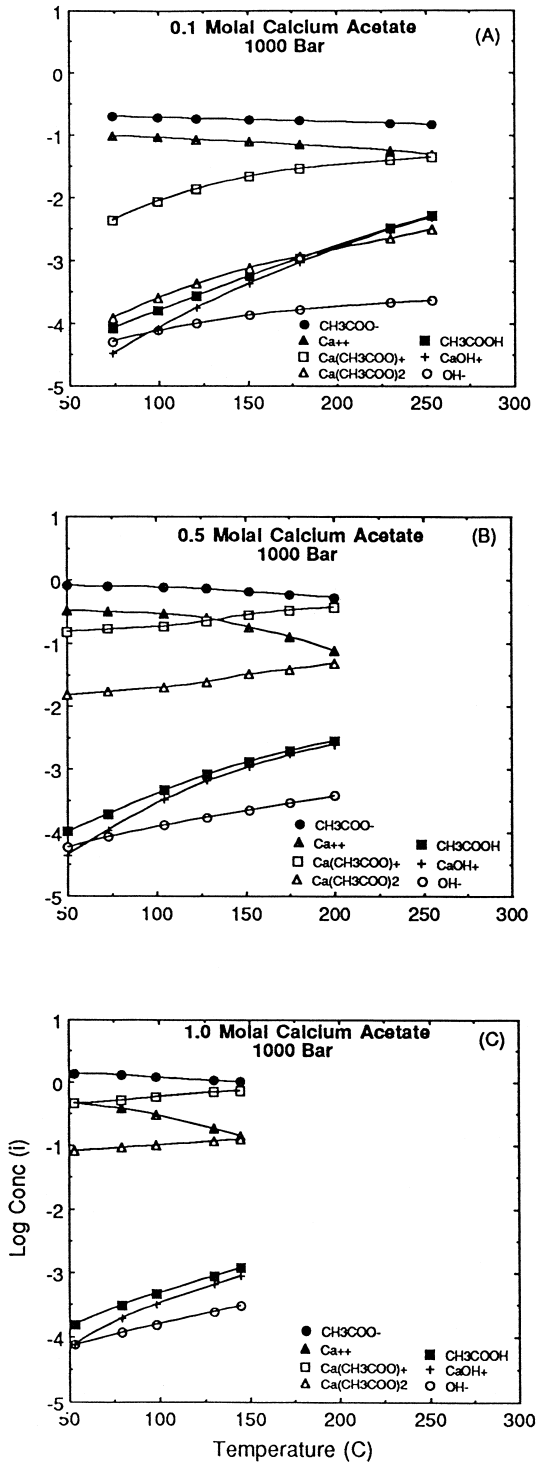

Fig. 12. Distribution of aqueous species of calcium acetate solutions as a function of temperature at 1000 bar pressure. (A) 0.1 molal calcium acetate solution; (B) 0.5 molal calcium acetate solution; and (C) 1.0 molal calcium acetate solution.

tion is consistent with the appearance of a third peak in the symmetric C–C stretch envelope at 248°C at 1000 bar and 304°C at 2000 bar for the experiments performed on 1.0 molal calcium acetate solutions (Fig. 9; Table 1).

5. Discussion

In order to model the chemical evolution of calcium acetate solutions as they are subjected to increasing temperature and pressure in the experiments discussed above, the chemical compositions of these fluids were computed using available experimentally and theoretically determined thermodynamic data. The principal source for these data was the data base for *SUPCRT92* (Johnson et al., 1992) updated with theoretically derived data from Shock et al. (1997). Association constants for the equilibria $Ca(CH_3COO)^+ + CH_3COO^- = Ca(CH_3COO)_2^\circ$ and $CaOH^+ + OH^- = Ca(OH)_2^\circ$ were assumed to be identical to those of the equilibria $Na^+ + Cl^- = NaCl^\circ$. This is justified by the relative similarity of these constants for a variety of salts including the first association constants of $CaCl_2$ and $MgCl_2$ (Frantz and Marshall, 1982). Values for the reaction $Ca^{2+} + CH_3COO^- = Ca(CH_3COO)^+$ were taken directly from Table 2 rather than from regressions of the data due to the dependence of the values of Log K on concentration. These data were used to compute the distributions of aqueous species for 0.1, 0.5, and 1.0 molal calcium acetate solutions as a function of temperature and pressure (Fig. 12). Calculations were performed using the program listed in the Appendix of Frantz et al. (1981). Activity coefficients were computed using the ''B-dot'' equation as described in the work of Helgeson (1969). The results, shown in Fig. 12, indicate that the experimental solutions were quite basic with the concentration of hydroxide increasing with increasing temperature and calcium acetate concentration. The calcium hydroxide species, $CaOH^+$ and $Ca(OH)_2^\circ$, are present in much smaller concentrations than the calcium acetate complexes and thus would be expected not to interfere with the interpretation of this spectral study. The species $Ca(OH)_2^\circ$, not shown in Fig. 12, occurs at concentrations less than 1.0×10^{-7} molal. Acetic acid appears to occur at concentrations several orders of magnitude less than that of acetate or $Ca(CH_3COO)^+$ and thus would not be expected to be resolvable in the Raman spectra. The neutral species, $Ca(CH_3COO)_2^\circ$, appears to be increasing in concentration with both increasing temperature and total calcium acetate concentration. Inspection of the trends in Fig. 12 indicate that it would be likely to expect the appearance in the Raman spectra of the neutral complex in 1.0 molal solutions at the higher experimental temperatures *of the study* as shown in Fig. 9. Appearance of this species would not be likely at lower total calcium acetate concentrations.

Acknowledgements

The project was supported by the Carnegie Institution of Washington and a grant from the Centre National de la Recherche Scientifique through its Programme International de Cooperation Scientifique (PICS #142).*[SB]*

References

Drummond, S.E., Palmer, D.A., 1986. Thermal decarboxylation of acetate: Part II. Boundary conditions for the role of acetate in the primary migration of natural gas and the transportation of metals in hydrothermal systems. Geochim. Cosmochim. Acta 50, 825–833.

Ellis, A.J., 1963. The ionization of acetic, propanoic, *n*-butyric, and benzoic acid in water, from conductance measurements up to 225°C. J. Chem. Soc. 1963, 2299–2310.

Frantz, J.D., 1981. High-pressure, high-temperature optical cell for Raman spectroscopy. Carnegie Inst. Washington, Year Book 80, 406–408.

Frantz, J.D., 1998. Raman spectra of potassium carbonate and bicarbonate aqueous fluids at elevated temperatures and pressures: comparison with theoretical simulations. Chem. Geol., in press.

Frantz, J.D., Marshall, W.L., 1982. Electrical conductance and ionization constants for calcium chloride and magnesium chloride in aqueous solutions at temperatures to 600°C and pressures to 4000 bars. Am. J. Sci. 282, 1666–1693.

Frantz, J.D., Popp, R.K., Boctor, N.Z., 1981. Mineral–solution equilibria: V. Solubilities of rock-forming minerals in supercritical fluids. Geochim. Cosmochim. Acta 45 (1), 69–77.

Frantz, J.D., Dubessy, J., Mysen, B.O., 1993. An optical cell for Raman spectroscopic studies in supercritical fluids and its application to the study of water to 500°C and 2000 bar. Chem. Geol. 106, 9–26.

Frantz, J.D., Dubessy, J., Mysen, B.O., 1994. Ion-pairing in aqueous $MgSO_4$ solutions along an isochor to 500°C and 11

kbar using Raman spectroscopy in conjunction with the diamond-anvil cell. Chem. Geol. 116, 181–188.

Giordano, T.H., 1989. Anglesite ($PbSO_4$) solubility in acetate solutions: the determination of stability constants for lead acetate complexes to 85°C. Geochim. Cosmochim. Acta 53, 359–366.

Giordano, T.H., 1993. Metal transport in ore fluids by organic ligand complexation. In: Pittman, E.D., Lewan, M.D. (Eds.), Organic Acids in Geological Processes. Springer-Verlag, New York, NY, 482 pp.

Helgeson, H.C., 1969. Thermodynamics of hydrothermal systems at elevated temperatures and pressures. Am. J. Sci. 267, 729–804.

Helgeson, H.C., Kirkham, D.H., 1974. Theoretical prediction of the thermodynamic behavior of aqueous electrolytes at high pressures and temperatures: II. Debye–Huckel parameters for activity coefficients and relative partial molal properties. Am. J. Sci. 274, 1199–1261.

Johnson, J.W., Oelkers, E.H., Helgeson, H.C., 1992. SUPCRT92: a software package for calculating the standard molal thermodynamic properties of minerals, gases, aqueous species, and reactions from 1 to 5000 bar and 0 to 1000°C. Comput. Geosci. 18 (7), 899–947.

Kaklhana, M., Kotaka, M., Okamoto, M., 1983. Vibrational analysis of acetate ion molecules and estimation of equilibrium constants for their hydrogen isotopic exchange reactions. J. Phys. Chem. 87, 2526–2535.

Kharaka, Y.K., Carothers, W.W., Rosenbauer, R.J., 1983. Thermal decarboxylation of acetic acid: implications for origin of natural gas. Geochim. Cosmochim. Acta 47, 397–402.

Klotz, I.M., 1964. Chemical Thermodynamics. W.A. Benjamin, New York, NY, 468 pp.

Long, D.A., 1977. Raman Spectroscopy. McGraw-Hill, New York, NY, 276 pp.

Palmer, D.A., Drummond, S.E., 1986. Thermal decarboxylation of acetate: Part I. The kinetics and mechanism of reaction in aqueous solution. Geochim. Cosmochim. Acta 50, 813–823.

Palmer, D.A., Drummond, S.E., 1988. Potentiometric determination of the molal formation constants of ferrous acetate complexes in aqueous solutions to high temperatures. J. Phys. Chem. 92, 6796–6800.

Quist, A.S., Marshall, W.L., 1968. Electrical conductances of aqueous sodium chloride solutions from 0 to 800° and to pressures of 4000 bars. J. Phys. Chem. 72, 684–703.

Seewald, J.S., Seyfried, W.E., 1991. Experimental determination of portlandite solubility in H_2O and acetate solutions at 100–350°C and 500 bars: constraints on calcium hydroxide and calcium acetate complex stability. Geochim. Cosmochim. Acta 55, 659–669.

Semmler, J., Irish, D.E., 1988. Vibrational spectral studies of solutions at elevated temperatures and pressures: 9. Acetic acid. J. Sol. Chem. 17, 805–824.

Semmler, J., Irish, D.E., Ozeki, T., 1990. Vibrational spectral studies of solutions at elevated temperatures and pressures: 12. Magnesium acetate. Geochim. Cosmochim. Acta 54, 947–954.

Shock, E.L., 1993. Application of thermodynamic calculations to geochemical processes. In: Pittman, E.D., Lewan, M.D. (Eds.), Organic Acids in Geological Processes. Springer-Verlag, New York, NY, 482 pp.

Shock, E.L., Koretsky, C.M., 1993. Metal-organic complexes in geochemical processes: calculation of standard partial molal thermodynamic properties of aqueous acetate complexes at high pressures and temperatures. Geochim. Cosmochim. Acta 57, 4899–4922.

Shock, E.L., Sassani, D.C., Willis, M., Sverjensky, D.A., 1997. Inorganic species in geologic fluids: correlations among standard molal thermodynamic properties of aqueous ions and hydroxide complexes. Geochim. Cosmochim. Acta 61 (5), 907–950.

Spohn, P.D., Brill, T.B., 1989. Raman spectroscopy of the species in concentrated aqueous solutions of $Zn(NO_3)_2$, $Ca(NO_3)_2$, $Cd(NO_3)_2$, $LiNO_3$, and $NaNO_3$ up to 450°C and 30 MPa. J. Phys. Chem. 93, 6224–6231.

Sverjensky, D.A., 1984. Oil field brines as ore-forming solutions. Econ. Geol. 79, 23–37.

Yang, M.M., Crerar, D.A., Irish, D.E., 1989. A Raman spectroscopic study of lead and zinc acetate complexes in hydrothermal solutions. Geochim. Cosmochim. Acta 53, 319–326.